ELSEVIER

Journal of Alloys and Compounds 342 (2002) 186–190

Journal of ALLOYS AND COMPOUNDS

www.elsevier.com/locate/jallcom

The square Fibonacci tiling

Ron Lifshitz*

School of Physics and Astronomy, Sackler Faculty of Exact Sciences, Tel Aviv University, Tel Aviv 69978, Israel

Abstract

We introduce the 2-dimensional square Fibonacci tiling and its generalization to higher dimensions as models for quasicrystals without 'forbidden' symmetries. We derive some of the basic mathematical properties of the tiling as well as calculate its diffraction pattern. We discuss the relevance of the Fibonacci tiling for quasicrystal research and for applications in other fields.
© 2002 Elsevier Science B.V. All rights reserved.

Keywords: Quasicrystals; Tiling; Symmetry; Fibonacci; Diffraction

1. Construction of the square Fibonacci tiling

Consider two identical Fibonacci grids, each consisting of an infinite set of lines whose inter-line spacings follow the well-known Fibonacci sequence of short (S) and long (L) distances

$$\ldots LSLLSLSLLSLSLLSLLSLSLLSLS \ldots \quad (1)$$

Superimpose the two grids at a 90° angle, as shown in Fig. 1, and you get a 2-dimensional quasiperiodic tiling with tetragonal point group symmetry $4mm$. This widely overlooked tiling, which we call the 'square Fibonacci tiling', is the subject of this paper. We shall describe its basic mathematical properties in Section 2, calculate its diffraction diagram in Section 3 and discuss its relevance to quasicrystal research in Section 4.

2. Properties of the square Fibonacci tiling

The mathematical properties of the square Fibonacci tiling are directly related, by way of its construction, to the well-known properties of the 1-dimensional Fibonacci sequence [1]. Consider first some of the trivial properties. The 1-d sequence consists of two 'tiles' or segments, S and L, whose lengths are proportional to 1 and the 'golden mean' $\tau = (1+\sqrt{5})/2 \simeq 1.618$, respectively. Consequently, the square Fibonacci tiling consists of three different tiles: a small square of dimensions 1×1, denoted by S^2; a large square of dimensions $\tau \times \tau$, denoted by L^2; and a rectangle of dimensions $1 \times \tau$, denoted by R. The 1-d sequence contains only two of the three possible types of '*vertices*' connecting pairs of tiles: LL and LS (or its mirrored version SL). The SS vertex never appears in the 1-d Fibonacci sequence. Consequently, in the square Fibonacci tiling there are only three allowed vertex configurations (to within rotations) as shown in Fig. 2(a). The

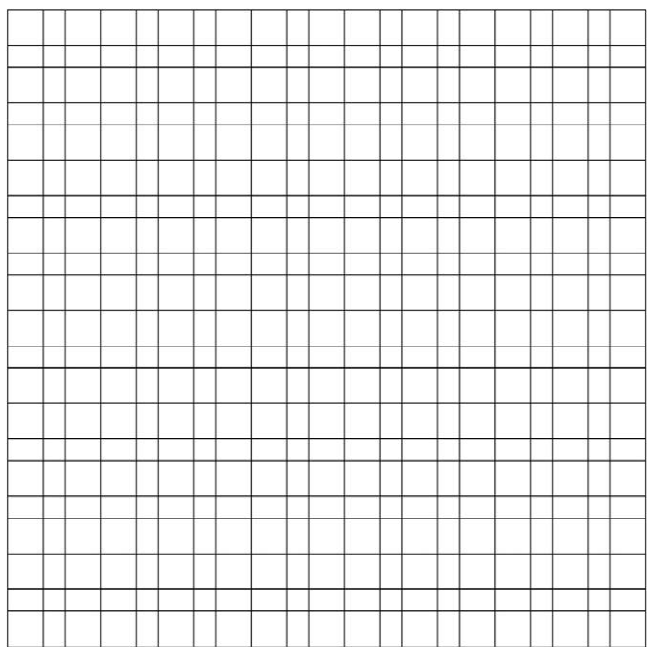

Fig. 1. The square Fibonacci tiling.

*Tel.: +972-3-640-5145; fax: +972-3-642-2979.
E-mail address: ronlif@post.tau.ac.il (R. Lifshitz).

0925-8388/02/$ – see front matter © 2002 Elsevier Science B.V. All rights reserved.
PII: S0925-8388(02)00169-X

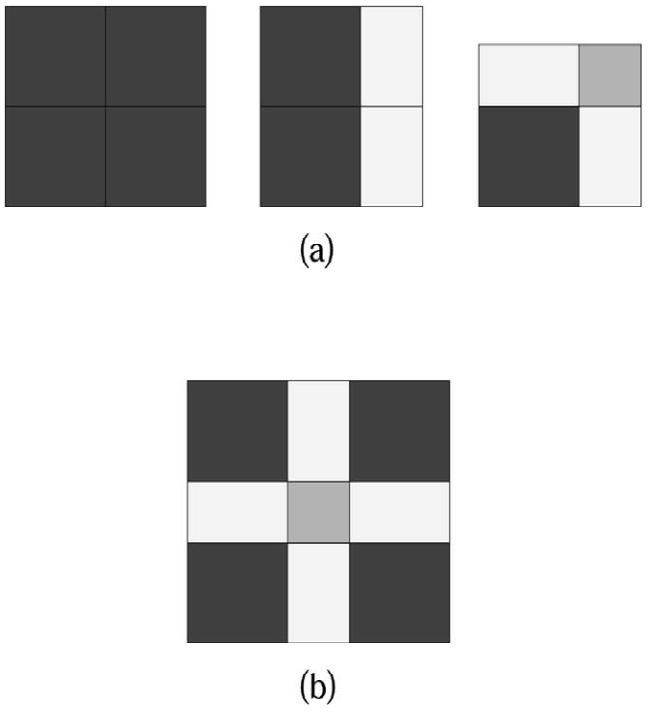

Fig. 2. (a) Atlas of allowed vertex configurations; (b) Minimal covering cluster.

1-d Fibonacci sequence has a 'minimal covering cluster' containing only three tiles, *LSL*. This means that one can cover the whole sequence by overlapping copies of this single cluster, or equivalently, that any tile in the sequence belongs to such a cluster. As a consequence, the square Fibonacci tiling has a minimal covering cluster of nine tiles, shown in Fig. 2(b).

Next, consider the various methods for generating the tiling. In addition to superimposing two Fibonacci grids, as we did in the initial construction of the tiling, one can directly generate the square Fibonacci tiling using any method that can be used to generate the 1-d Fibonacci sequence. It can be generated by the cut-and-project method from 4-dimensional space; it can also be generated using the dual multi-grid method; both in an obvious generalization of the procedure used to generate the 1-d Fibonacci sequence. More interesting is to generate the tiling using substitution, or inflation, rules. The substitution rules for each of the tiles in the square Fibonacci tiling, shown in Fig. 3, follow immediately from the substitution rules for the 1-d sequence: $S \rightarrow L$, $L \rightarrow LS$.

Using the substitution rules for the tiling one can easily calculate the tile frequencies, namely, what fraction $P(L^2)$ of the tiles are large squares, what fraction $P(S^2)$ are small squares, and what fraction $P(R)$ are rectangles. This is done, as usual, by examining the components of the eigenvector, corresponding to the largest eigenvalue of the substitution matrix [1]. The substitution matrix, considering the horizontal and vertical rectangular tiles as the same tile, is simply

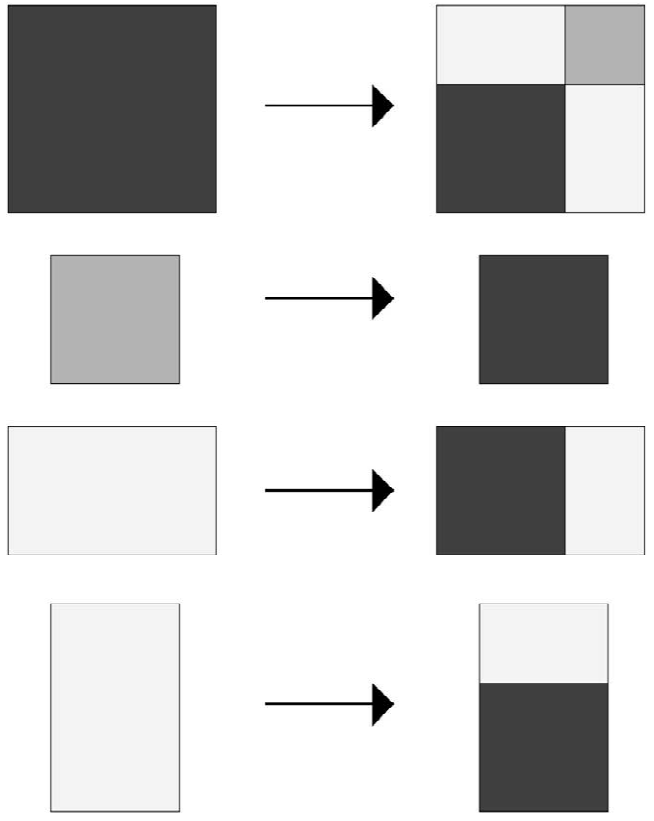

Fig. 3. Substitution rules for the square Fibonacci tiling.

$$M = \begin{pmatrix} 1 & 1 & 1 \\ 1 & 0 & 0 \\ 2 & 0 & 1 \end{pmatrix}. \tag{2}$$

The eigenvalues of M are $\lambda_1 = \tau^2$, $\lambda_2 = \tau^{-2}$ and $\lambda_3 = -1$. The eigenvector of the largest eigenvalue λ_1 is proportional to

$$\mathbf{v}_1 = \begin{pmatrix} \tau^2 \\ 1 \\ 2\tau \end{pmatrix}. \tag{3}$$

Thus, there are τ^2 times as many L^2 tiles as there are S^2 tiles, and there are 2τ times as many R tiles as there are S^2 tiles. Dividing the components of $\mathbf{v}_1$ by their sum $\tau^2 + 1 + 2\tau = \tau^4$, one gets the tile frequencies: $P(L^2) = \tau^{-2}$, $P(S^2) = \tau^{-4}$ and $P(R) = 2\tau^{-3}$. It is left as an exercise for the reader to show that one can obtain the same result by using the knowledge that in the 1-d Fibonacci sequence there are τ times as many L's as there are S's.

Finally, note that the square Fibonacci tiling also has unique composition rules, meaning that the substitution rules of Fig. 3 can uniquely be iterated backwards, as shown by thick lines in Fig. 4. Thus, the vertices of the square Fibonacci tiling contain as a subset another square Fibonacci tiling whose tiles are scaled by a factor of τ (tile areas are scaled by a factor of $\lambda_1 = \tau^2$). The square Fibonacci tiling inherits its τ-scaling or inflation symmetry

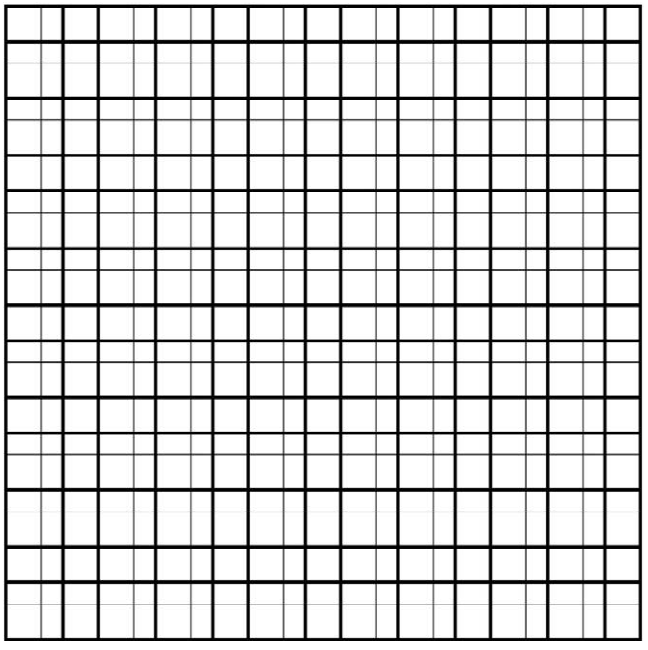

Fig. 4. Demonstration of the τ scaling symmetry of the square Fibonacci tiling.

directly from the 1-d Fibonacci sequences from which it is constructed.

3. Diffraction pattern

Now, associate an 'atom' in the form of a δ-function scatterer with each vertex of the square Fibonacci tiling, and calculate the Fourier transform. As a first step note that one can label all the vertices of the tiling by a pair of successive integers (n,m), starting arbitrarily from a vertex labeled (0,0) and counting the number of tiles n crossed in the x-direction and the number of tiles m crossed in the y-direction. The position $\mathbf{r}_{(n,m)}$ of the vertex (n,m) can be specified analytically by recalling that the position of the nth vertex x_n of the 1-d Fibonacci sequence is given by the function

$$x_n = \mathscr{F}ib(n) = \left\| \frac{n}{\tau} \right\| \tau + \left(n - \left\| \frac{n}{\tau} \right\| \right), \tag{4}$$

where $\|z\|$ is the largest integer $\leq z$. It then follows that

$$\mathbf{r}_{(n,m)} = \mathscr{F}ib(n)\hat{x} + \mathscr{F}ib(m)\hat{y}, \tag{5}$$

where $\hat{x}$ and $\hat{y}$ are unit vectors in the x- and y-directions. This can easily be generalized to an arbitrary number of dimensions d, where the position of the vertex $(n_1, \ldots n_d)$ of the d-dimensional Fibonacci tiling is given by

$$\mathbf{r}_{(n_1, \ldots n_d)} = \mathscr{F}ib(n_1)\hat{x}_1 + \ldots + \mathscr{F}ib(n_d)\hat{x}_d. \tag{6}$$

Recall also that for a 1-dimensional density of δ-function scatterers, arranged according to the Fibonacci sequence

$$\rho^{(1)}(x) = \sum_n \delta(x - \mathscr{F}ib(n)), \tag{7}$$

the Fourier transform

$$\hat{\rho}^{(1)}(k) = \int \mathrm{d}x\, \mathrm{e}^{ikx} \rho^{(1)}(x) = \sum_n \mathrm{e}^{ik\mathscr{F}ib(n)} \tag{8}$$

can be calculated analytically via the cut-and-project description [1,2] to give

$$\hat{\rho}^{(1)}(k) = \sum_{h_1,h_2} \tau^2 \frac{\sin K^{\perp}_{h_1,h_2}}{K^{\perp}_{h_1,h_2}} \delta(k - (h_1[\tau a^*] + h_2[a^*])). \tag{9}$$

The diffraction diagram of the Fibonacci sequence contains Bragg peaks whose positions are located on a reciprocal lattice of rank 2, generated by all integral linear combinations of the two wave vectors $a^* = 2\pi/(\tau + 2)$ and τa^*. The amplitude of each peak depends on the so-called 'perpendicular wave vector'

$$K^{\perp}_{h_1,h_2} = \frac{\tau^2}{2}(h_2[\tau a^*] - h_1[a^*]). \tag{10}$$

The key to calculating the Fourier transform of the square Fibonacci tiling (or any of its d-dimensional generalizations) is the fact that the x and y coordinates of the vertex positions $\mathbf{r}_{(n,m)}$ are independent of each other. The calculation in 2 or higher dimensions decomposes into independent 1-dimensional calculations. If one takes a set of point-like scatterers on the vertices of the 2-d square Fibonacci tiling

$$\rho^{(2)}(x,y) = \sum_{n,m} \delta(x - \mathscr{F}ib(n))\delta(y - \mathscr{F}ib(m)), \tag{11}$$

then the Fourier transform is simply

$$\begin{aligned} \hat{\rho}^{(2)}(k_x,k_y) &= \int\int \mathrm{d}x\, \mathrm{d}y\, \mathrm{e}^{i(k_x x + k_y y)} \rho^{(2)}(x,y) \\ &= \left(\sum_n \mathrm{e}^{ik_x \mathscr{F}ib(n)} \right) \left(\sum_m \mathrm{e}^{ik_y \mathscr{F}ib(m)} \right) \\ &= \hat{\rho}^{(1)}(k_x)\hat{\rho}^{(1)}(k_y). \end{aligned} \tag{12}$$

The two coordinates separate, giving a 2-d Fourier transform which is the product of two 1-d Fourier transforms of the form (9). In d-dimensions one similarly gets

$$\hat{\rho}^{(d)}(k_1, \ldots k_d) = \hat{\rho}^{(1)}(k_1) \cdots \hat{\rho}^{(1)}(k_d). \tag{13}$$

The Fourier transform of the square Fibonacci tiling is shown in Fig. 5, where amplitudes are proportional to circle radii. Note that the resulting diffraction diagram is of rank 4. It is generated by the 4 wave vectors $a^*\hat{x}$, $\tau a^*\hat{x}$, $a^*\hat{y}$ and $\tau a^*\hat{y}$. The peak intensities associated with these 4 vectors are comparable, indicating that the structure is *not* an incommensurately modulated crystal. The Fourier transform also confirms the 4*mm* point-group symmetry as well as the τ-scaling symmetry of the tiling.

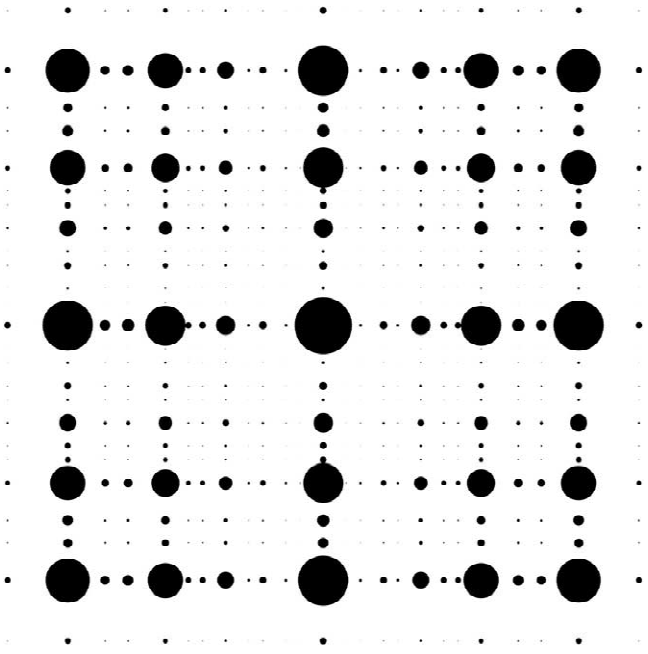

Fig. 5. Fourier transform of the square Fibonacci tiling. The amplitude at each point is proportional to the radius of the circle.

4. Discussion: Is the square Fibonacci tiling good for anything?

I would like to use the last section to argue that the square Fibonacci tiling, as well as its 3-dimensional cubic version, are both relevant and potentially useful for research in the field of quasicrystals. If this is so, the reader might wonder why these tilings have been ignored up until now. I imagine that the reason is that according to the prevailing (though unofficial) definition [3–5], a quasicrystal is required to have some 'forbidden' symmetry, incompatible with periodicity—at least one axis of n-fold symmetry with $n=5$ or $n>6$. I have argued elsewhere [6] that this requirement should officially be removed from the definition of quasicrystals. The existence of the square Fibonacci tiling supports this argument. It is a quasiperiodic tiling with many of the features normally associated with standard tiling models of quasicrystals like the Penrose tiling. It has a finite number of tiles with definite tile frequencies and a finite number of vertex configurations; it can be generated by most of the standard methods for generating quasiperiodic tilings; its diffraction diagram contains Bragg peaks with no clear subset of main-reflections; and most notably, it has τ-inflation symmetry. Like the proverbial bird that looks like a duck, walks like a duck, quacks like a duck, and is therefore a duck—the square Fibonacci tiling *is* a model quasicrystal even though it has no 'forbidden' symmetries.

To the best of my knowledge, no alloys or real quasicrystals exist with the structure of the square or cubic Fibonacci tilings. Nevertheless, there have been experimental reports of cubic quasicrystals [7,8] as well as tetrahedral [9], tetragonal [10], and possibly also hexagonal [11] quasicrystals. One of the cubic quasicrystals [8], a Mg–Al alloy, is even reported to have inflation symmetry involving irrational factors related to $\sqrt{3}$. The structure of this alloy might have some features in common with the cubic Fibonacci tiling.

Even if there are no real quasicrystals exhibiting the structure of the square Fibonacci tiling, it still does not imply that the tiling is experimentally irrelevant. In recent years, we have come to know a number of experimental applications where one creates artificial quasicrystals. One example is in the field of photonic crystals [12], with the aim of producing novel photonic band-gap materials. Another example is in the field of non-linear optics [13], with the aim of achieving third- and fourth-harmonic generation in a single crystal. In both of these examples, it would be beneficial to make artificial quasicrystals with the structure of the square Fibonacci tiling.

Finally, I would like to promote the square Fibonacci tiling and its cubic version as useful theoretical tools. They can be used to explore novel quasiperiodic order such as magnetic order [14] and color symmetry [15]. More importantly, they can be used to calculate physical properties of quasicrystals such as electronic, photonic, and phononic structure and transport, as well as phason and defect dynamics. In all cases, on a model much simpler than the standard 2-d and 3-d tiling models of quasicrystals, where, as in the example of the calculation of the Fourier transform (12), it is expected that the coordinates will easily separate.

Acknowledgements

I thank Ma'ayan Honig for participating in some of the explorations of the square Fibonacci tiling. This research is supported by the Israel Science Foundation (Grant No. 278/00).

References

[1] See, for example M. Senechal, Quasicrystals and Geometry, Cambridge Univ. Press, Cambridge, 1996.
[2] V. Elser, Phys. Rev. B32 (1985) 4892.
[3] P.M. Chaikin, T.C. Lubensky, Principles of Condensed Matter Physics, Cambridge Univ. Press, Cambridge, 1995, p. 680.
[4] S. van Smaalen, Cryst. Rev. 4 (1995) 79.
[5] Ref. [1], p. 31 (but see the comment on p. 33).
[6] R. Lifshitz, preprint (cond-mat/0008152).
[7] Y.C. Feng, G. Lu, H.Q. Ye, K.H. Kuo, R.L. Withers, G. van Tendeloo, J. Phys. Condens. Matter. 2 (1990) 9749.
[8] P. Donnadieu, H.L. Su, A. Roult, M. Harmelin, G. Effenberg, F. Aldinger, J. Phys. I. France 6 (1996) 1153.
[9] P. Donnadieu, J. Phys. I. France 4 (1994) 791.
[10] Z.H. Mai, L. Xu, N. Wang, K.H. Kuo, Z.C. Jin, G. Cheng, Phys. Rev. B40 (1989) 12183.

[11] H. Selke, U. Vogg, P.L. Ryder, Phys. Status Solidi 141 (A) (1994) 31.
[12] M. Hase, M. Egashira, N. Shinya, H. Miyazaki, K.M. Kojima, S. Uchida, J. Alloys Comp. 342 (2002) 455.
[13] K. Fradkin-Kashi, A. Arie, IEEE J. Quantum Electron. 35 (1999) 1649;
K. Fradkin-Kashi, A. Arie, P. Urenski, G. Rosenman, Phys. Rev. Lett. 88 (2002) 023903.
[14] R. Lifshitz, Phys. Rev. Lett. 80 (1998) 2717;
R. Lifshitz, Mat. Sci. Eng. 294 (A) (2000) 508.
[15] R. Lifshitz, Rev. Mod. Phys. 69 (1997) 1181.